J-Researchers

Journal of Civil Engineering Researchers

Journal homepage: www.journals-researchers.com

Evaluation of Mechanical Properties of Activated Alkali Concrete Based on Non-Destructive Ultrasonic Wave Velocity Testing

Mohammadhossein Mansourghanaei[a,*]

[a] Ph.D. in Civil Engineering, Department of Civil Engineering, Chalous Branch, Islamic Azad University, Chalous, Iran

ABSTRACT

In this experimental study, a mixed design of ordinary concrete containing Portland cement (OPCC) with a grade of 500 kg/m3 and a design of activated alkali concrete (AAC) based on granulated blast furnace slag (GBFS) were made. In order to investigate the mechanical properties, ultrasonic pulse velocity (UPV) tests were performed on concrete designs at a temperature of 21 ℃ at curing ages of 7, 28 and 90 days. The results indicated that the UPV improved with increasing curing age in OPCC and AAC samples. In this regard, in OPCC, the minimum (4128 m/s) and maximum (6179 m/s) UPV was obtained at curing ages of 7 and 90 days, respectively, which had a superiority of 49.68% at the age of 90 days. In AAC, the minimum (4723 m/s) and maximum (5531 m/s) UPV was achieved at 7 and 90 days of curing, respectively, with a 17.1% advantage at 90 days. At 90 days of curing (as the optimum age), the UPV in AAC decreased by 11.71% compared to OPCC at the same age. The results of the analysis of scanning electron microscope (SEM) images on concrete samples in this study were in complete agreement with the UPV test results.

ARTICLE INFO

Received: June 08 , 2026
Accepted: June 28 , 2026

Keywords:
Alkali Activated Concrete
Ultrasonic Pulse Velocity
Scanning Electron Microscopy
Hydrated Gels
Concrete Technology

DOI: 10.66224/JCER.8.3.9
DOR: 20.1001.1.22516530.1399.11.4.1.1

1. Introduction

In order to develop national security and passive defense in the field of civil engineering infrastructure, a lot of experimental work has been done to produce structural concrete for strategic and sensitive centers of the country [1-3]. The strength of reinforced concrete structures of these centers plays an important role in reducing destruction and human injuries caused by enemy defense operations. Improving the strength of concrete can be achieved through the type of materials used in its mixture composition [4-10].

The human hearing frequency is in the range of 20 Hz to 20 kHz. Waves below this range are called infrasound waves, which are not audible to humans. Frequencies above 20 kHz, which are not in the range of human hearing, are called ultrasound waves. Ultrasound waves are a type of sound wave that is inaudible to humans. In recent decades, the speed of UPV has found a wide perspective in various sciences. UPV are produced by special ultrasonic devices such as magnetic or piezoelectric transducers. One of the important applications of producing this type of waves is its use in determining the quality and density of concrete as a non-destructive test in civil engineering science [3-5]. Various standards have been defined for performing ultrasonic testing in concrete. In this test, waves are guided into the concrete through a transducer and acoustics, and the high speed of the waves indicates

* Corresponding Author. Tel: +989121712070; E-Mail: Mhm.Ghanaei@Gmail.Com

high density and compaction in the hardened concrete composition.

Low density in OPCC has always created many challenges in the mechanical properties and durability of concrete. On the other hand, the use of ordinary cement in concrete has led to environmental problems due to the consumption of mineral resources, the consumption of fossil fuels, and the emission of toxic carbon dioxide gas due to cement production in factories [1-10]. As research has shown, cement factories are responsible for the emission of about 5% of the total carbon dioxide entering the Earth's atmosphere [11]. In order to solve these problems in OPCC, researchers have introduced fly ash, metakaolin, blast furnace slag, and other pozzolans as suitable alternatives to cement in OPCC [12-14]. Replacing these pozzolans with cement results in the production of AAC, which is effective in reducing environmental pollution and increases the mechanical properties [1,2] of concrete, and also reduces the extensive need for cement [15,16]. The amount of carbon dioxide produced in the AAC production process is much lower than that of OPCC production [17]. The use of blast furnace slag instead of cement can improve the strength of concrete and reduce the increasing demand for cement in concrete [18,19]. Activation of blast furnace slag with alkali activated solution (AAS) to produce alkali-activated slag cement has been studied for the past few decades [20]. By adding blast furnace slag to the concrete mix, the pore structure in the concrete is optimized and the pore size distribution is more appropriate, the interfacial transition zone (ITZ) is denser and the strength and resistance aspects of the concrete are gradually increased, in other words, the development of strength and durability is closely related to the evolution of the pore structure and ITZ in activated AAC [21]. Blast furnace slag contains aluminosilicate particles with high pozzolanic properties, the chemical combination of these materials with the AAS leads to the production of a large volume of hydrated gels such as hydrated calcium silicate called tobermorite gel (C-S-H) and hydrated calcium aluminum silicate called tobermorite-like gel (C-A-S-H) and hydrated sodium aluminum silicate called tobermorite-like gel (N-A-S-H) in the concrete mix. These gels, with their high adhesive and filling properties, are the main factor in creating density and strength in hardened concrete. In this experimental study, the quality and density of OPCC and AAC were measured using ultrasound waves. The goals and innovations of this experimental study through the production of AAC can be summarized as follows:

1- The mechanical and microstructural properties of AAC are improved compared to OPCC.

2- Helping to reduce the volume of toxic carbon dioxide emissions compared to OPCC production, according to the report provided by other researchers in this regard.

3- Helping to maintain environmental health by using (in the composition of AAC) slag accumulated in iron smelting plants, known as environmentally harmful materials.

4- Conserving and reducing the consumption of consumable mineral resources that are used as main materials during the ordinary cement manufacturing process.

5- Conserving and reducing the consumption of fossil fuels that are used as fuel in ordinary cement production plants.

2. Matrials

In this experimental study, Portland cement type 2, produced by Gilan Sabz Cement Industries Factory (Dilman), with a density of 3250 kg/m3 and a specific surface area of 3000 to 3200 cm2/g, which was produced under the ISIRI 389 standard, was used. Slag from the blast furnace, produced by the Isfahan Iron Smelting Factory, with a density of 2750 kg/m3, a specific surface area of 2200 cm2/g, and a bulk density of 960 kg/m3, was used under the ASTM C989/C989M standard. The chemical characteristics of GBFS and Portland cement are shown in Table 1. The water used to prepare lime water and make the mixture design in the present study was from the drinking water of Lahijan city. This type of water has a pH in the range of 6.5 to 7.5 and a density of 1000 kg/m3. According to Section 2-4-10-9 and 3-4-10-9 of the fourth edition of the National Building Regulations of Iran, water that is potable, has no distinct taste or odor, and is clean and clear can be used in concrete without testing, unless previous records indicate that this type of water is unsuitable for concrete. The aggregate used in preparing the concrete mix design in this experimental study is synthetic and based on the requirements of the ASTM C33 standard, obtained from sand and gravel factories in Lahijan city. Some of the characteristics of the aggregate used in this study are shown in Table 2. Research has shown that fresh AAC has poorer performance compared to fresh OPCC due to the high viscosity of the AAC. To solve this problem, a polycarboxylate-based superplasticizer is the best option, often due to the strong bonds between positively charged calcium and negatively charged polycarboxylate [22]. In this regard, polycarboxylate normal superplasticizer (PCNS), a product of Durochem Middle East Company, was used based on the characteristics in Table 3. The AAS used in this study was a mixture of sodium silicate and sodium hydroxide solution with a weight ratio of 2.5, which was used with a combined density of 1483 kg/m3, in order to maintain the fluidity and performance of the concrete [1-

10]. Some of the characteristics of the AAS used in this study are shown in Table 4.

Table 1.
Chemical Characteristics of GBFS and Portland Cement (%)

Component	GBFS	Portland Cement
SiO_2	29.2	21.3
Al_2O_3	19.4	4.7
Fe_2O_3	5.8	4.3
CaO	38.6	62.7
MgO	2.8	2.1
SO_3	2.6	2
K_2O	0.1	0.65
Na_2O	0.2	0.18
TiO_2	0.6	-
LOI	0.3	1.84

Table 2
Aggregate Specifications

Concrete Aggregates	Gravel	Sand
Minimum Diameter	4.75 (mm)	75 (µm)
Maximum Diameter (mm)	19	4.75
Modulus of Elasticity (mm)	5.7	2.85
Density (kg/m3)	2750	2650
Water Absorption (%)	2.2	2.9

Table 3.
PCNS Specifications

Chemical Formula	Normal Polycarboxylate
Physical Condition	Liquid
Color	Light Brown
Density (kg/m3)	1100
Consumption Standard	ASTM C494
pH	About 7

3. Mix Design

There is no separate standard for the mix design of AAC, therefore, following some experimental research [1,2,23], the mix design of AAC was prepared and adjusted in accordance with the standard for preparing OPCC under the recommendation of the ACI Committee 211.1-89 based on Table 5.

4. Construction and Curing

Initially, the materials used were weighed according to Table 4 of the mixing plan, and then the dry materials including cement (or GBFS) and aggregate were poured into a rotating electric mixer, and the mixing process lasted for 1.5 minutes. Next, the wet materials including water (or AAS) were added to the mixture, and the mixing of the materials lasted for another 2.5 minutes. Then, the fresh concrete mixture was poured into foil-lined and oiled metal molds in three stages. In this regard, in order to compact the concrete sample, 25 blows were applied to the concrete mixture with a special rod in each stage. Finally, the molds containing the concrete samples were kept in a dry environment at a temperature of 21 ℃ for 24 hours. After this time, the samples were demoulded, and the OPCC samples were kept and cured in lime water at a temperature of 21 ℃until the test age. After molding, the AAC samples were subjected to heat treatment in a furnace at 60 ℃for 48 hours to improve the strength of this type of concrete. After this time, the concrete samples were removed from the furnace and stored and cured in a dry environment at 21 ℃ until the test time. In terms of heat treatment in alkali-activated concrete, research has shown that AAC samples subjected to heat treatment in the range of 50 to 70 ℃have higher strength than samples cured at 20 ℃[1,2,24].

Table 4.
AAS Specifications

Formula	NaOH	Na2SiO3
Color	Colorless	Colorless
Molarity (mol/m3)	12	12
Density (kg/m3)	2130	2400
Modulus of Elasticity (GPa)	3.3	-
Melting Temperature (C)	318	1088
Molar Mass (gr/mol)	39.99	122.06
*	-	2.4
**	-	47

* Molar Weight Ratio of Silicate to Sodium

** Molar Weight Ratio of Silicate to Water

5. Standards and Test Method

In this study, UPV test in concrete was measured under ASTM C597 standard on cubic samples with dimensions of 10×10×10 cm at room temperature and high temperature, with a Dundee type device with a vibration frequency of 55 kHz and an accuracy of 0.1 and ±2% of the wave travel time. In this regard, at a curing age of 90 days, the surface dimensions of the samples that were in contact with the mold bottom were measured by calipers, then appropriate acoustic coupling was achieved between the concrete surface (smooth surfaces that were in contact with the mold faces) and the transducer surface to remove air pockets through Vaseline on the surface of the samples. After determining the time for the waves to pass through the concrete sample, the UPV value was obtained in meters per second using the relationships in the mentioned standard. SEM image analysis was performed on concrete at a curing age of 90 days at a temperature of 21 ℃ using a FEI Quanta200 SEM. In this regard, a crushed concrete sample was placed in the device and images were recorded at the desired magnification and then microstructurally examined.

6. Interpretation and Test Results

6.1. Interpretation and Results of UPV Test

The results of the non-destructive UPV test on concrete samples obtained in this study are shown in the diagram in Figure 1. Based on these results, it is observed that increasing the curing age of concrete has improved the results. These results have also been obtained in other research (in the field of AAC) [3-5]. In this regard, in OPCC the speed of UPV has increased from 4128 m/s at a curing age of 7 days to 6179 m/s at a curing age of 90 days, which has achieved an improvement of 49.68% at a curing age of 90 days. In alkali-activated concrete, the UPV value has increased from 4723 m/s at a curing age of 7 days to 5531 m/s at a curing age of 90 days, which has achieved an improvement of 17.1% at a curing age of 90 days. Research shows that UPV values in OPCC at a curing age of 90 days have the least changes compared to curing ages of 7 and 28 days, due to the completion of a large part of the polymerization process (hydration or polymerization) [25].

The UPV value in AAC at 7 and 90 days of curing decreased by 6.81 and 10.48 percent, respectively, compared to OPCC at the corresponding curing ages. This can be attributed to the microcracks in AAC resulting from thermal curing at 60 ℃, which caused a lack of compaction in the microstructure of the concrete, which delayed the UPV values in the concrete sample.

In this regard, research by other researchers has shown that in AAC, due to curing in a dry furnace environment, a series of microcracks are formed in the concrete, which causes the concrete to be removed from complete integrity, which causes the transmission of UPV at a higher speed, and this causes the speeds obtained in AAC to be slightly lower than in OPCC. Of course, the presence of these cracks is very small in size and only affects the UPV value and will not have much effect on other properties of the samples [2-5,26]. On the other hand, the speed of the polymerization process in completing the production of hydrated gels and creating density in the microstructure of the concrete plays an effective role in the UPV value in concrete. GBFS particles contain abundant silica-aluminate materials that, when combined with chemical solutions, produce hydrated gels such as C-S-H, C-A-S-H, and N-A-S-H.

These gels provide strength to hardened concrete by filling pores, cavities, cracks, and bonding in the ITZ at the interface between cement paste and aggregate. In this regard, research has shown that in the geopolymerization reaction based on the geopolymerization mechanism, by converting CH into hydrated gel such as C-S-H, the microstructures in the concrete are condensed and cause homogeneity of the concrete [27].

The IS 13311-1 standard [28] shows the range of concrete quality in the UPV test and has been used in numerous studies (in the field of OPCC and AAC) [2-5,7,29]. This standard classifies concrete quality into four levels: Doubtful with a speed below 3000 m/s, Moderate with a speed of 3000 to 3500 m/s, Good with a speed of 3500 to 4500 m/s, and Excellent with a speed of more than 4500 m/s. In this regard, for the OPCC obtained from the present study, the concrete sample at the age of 7 days of curing is in the good quality range and at the ages of 28 and 90 days of curing is in the excellent quality range of the chart. In alkali-activated concrete, the concrete samples at all curing ages of 7, 28, and 90 days are in the excellent quality range of the chart.

According to the IS 13311-1 standard, as long as the UPV values are in the “Excellent” category, it means that the concrete in question does not have cracks or large holes that affect the integrity of the sample structure [30].

Table 5. Concrete Mix Design Specifications

Concrete Type	Materials / Quantity	Cement	GBFS	Water	Sand	Gravel	PCNS*	Density (kg/m3)	Curing
OPCC	kg/m3	500	0	225	1000	765	7	2497	Water
	%	20.02	0	9.01	40.04	30.63	0.0028		
AAC	kg/m3	0	500	225	1000	762.63	7	2494	Heat + dry Environment
	%	0	20.04	9.19	40.08	30.57	0.0028		

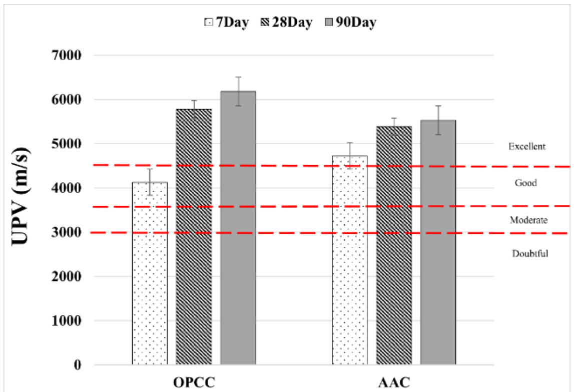

Figure 1. UPV Test Results

6.2. SEM Analysis Results

In this experimental study, the results of the analysis of SEM images at a scale of 100 µm are shown in Figure 2. In general, the images of the microstructure of OPCC paste and AAC can be divided into several parts as follows [1-5].

1) Includes hydrated gels resulting from the polymerization and geopolymerization process, which are mainly observed as dark areas in the figures.

2) Unhydrated clinker grains and particles resulting from the presence of impurities in the raw materials, which are mainly observed as white areas in the figures.

3) Cracks and microcracks in the mixture due to thermal shrinkage resulting from thermal treatment and polymerization and geopolymerization heat, due to the high content of Portland cement and GBFS in the concrete mixture.

4) Interlayer capillary pores and pores in the structure of hydrated gels and interfacial capillary pores and pores in the transition areas.

5) Other particles not participating in the chemical process.

In the images of the OPCC sample, the density of hydrated gels is seen in appropriate amounts, but the tree structure due to the incomplete polymerization process is also present in the images. The fine white particles are caused by unhydrated clinker grains and impurities in the raw materials, which have a negative effect on the density of the microstructure in the concrete sample. In AAC, due to the production of various hydrated gels with a larger volume than in the OPCC mixture, better density of these gels is seen in the concrete mixture. This has caused the volume and size of pores and cavities to be reduced, but the microcracks in this type of concrete, which have a negative effect on the UPV results in the concrete, are caused by the thermal treatment of the AAC under a temperature of 60 ℃. These microcracks delay the UPV in the concrete.

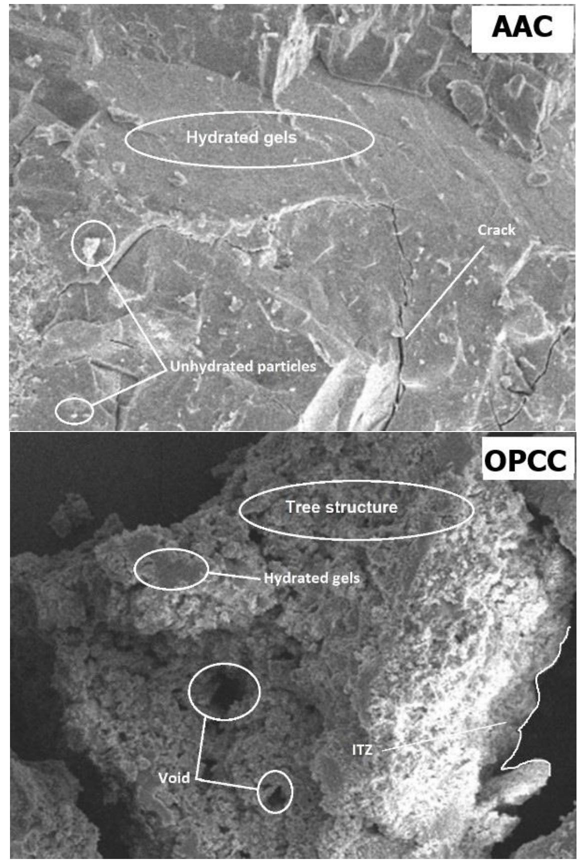

Figure 2. SEM Images of Concrete

7. Conclusion

In this experimental study, a mix design of OPCC and a mix design of AAC were made in order to investigate the UPV amount by non-destructive method. Next, SEM images were taken from the microstructure of hardened concrete and the results were evaluated. The results of this study are presented as follows.

1- In OPCC, the minimum (4128 m/s) and maximum (6179 m/s) UPV amount were obtained at 7 and 90 days curing age, respectively, with a difference and superiority of 49.68% at 90 days curing age compared to 7 days curing age.

2- In alkali-activated concrete, the minimum (4723 m/s) and maximum (5531 m/s) UPV values were obtained at 7 and 90 days of curing, respectively, with a difference and advantage of 1.17% at 90 days of curing compared to 7 days of curing.

3- At 90 days of curing (as the optimal age), the UPV value in AAC decreased by 11.71% compared to OPCC.

This is mainly due to the presence of microcracks in the microstructure of AAC due to the thermal curing of the concrete at 60 ℃.

4- The results of SEM analysis on concrete samples in this study were in complete overlap and agreement with the UPV test results

8. Reference

[1] Mansourghanaei M, Biklaryan M, Mardookhpour A. “Durability and mechanical properties of granulated blast furnace slag based geopolymer concrete containing polyolefin fibers and nano silica.” KSCE J Civ Eng 28.1 (2024): 209-219. https://doi.org/10.1007/s12205-023-1034-x

[2] Mansourghanaei M, Biklaryan M, Mardookhpour A. “Experimental study of the effects of adding silica nanoparticles on the durability of geopolymer concrete.” Aust J Civ Eng 22.1 (2024): 81-93. https://doi.org/10.1080/14488353.2023.2212911

[3] Mansourghanaei M, Biklaryan M, Mardookhpour A. “Experimental study of properties of green concrete based on geopolymer materials under high temperature.” Civ Eng Infrastruct J 56.2 (2023): 365-379. https://doi.org/10.22059/ceij.2023.355095.1923

[4] Mansourghanaei M, Mardookhpour A. “Analysis of the Numerical Results Obtained from the Experimental Examination of the Mechanical Properties of Geopolymer Concrete.” Numer Methods Civ Eng 9.1 (2024): 31-41. https://doi.org/10.52547/nmce.9.1.31

[5] Mansourghanaei M, Biklaryan M, Mardookhpour A. “Experimental Study of Mechanical Properties of Slag Geopolymer Concrete under High Temperature, Used in Road Pavement.” Int J Transp Eng 11.1 (2023): 1371-1385. https://doi.org/10.22119/ijte.2023.401879.1699

[6] Mansourghanaei M, Mardookhpour A. “Investigating the Properties of Environmentally Friendly Green Concrete (Geopolymer) Under High Temperature.” Sustainable Earth Trends 3.4 (2023): 62-69.

[7] Mansourghanaei M, Biklaryan M, Mardookhpour A. “Experimental Study of Modulus of Elasticity, Capillary absorption of water and UPV in Nature-Friendly Concrete Based on Geopolymer Materials.” Int J Adv Struct Eng 12.2 (2022): 607-615.

[8] Mansourghanaei M. “Experimental Evaluation of The Impact Resistance of Alkali-Activated Slag Concrete Under High Temperature.” J Civ Eng Res 6.3 (2024): 47-53.

[9] Mansourghanaei M. “Investigating the Mechanical and Durability Properties of Geopolymer Concrete Based on Granulated Blast Furnace Slag as Green Concrete.” J Civ Eng Res 5.3 (2023): 24-34.

[10] Mansourghanaei M. “Evaluation of Mechanical Properties and Microstructure of Pozzolanic Geopolymer Concrete Reinforced with Polymer Fiber.” J Civ Eng Res 5.2 (2023): 1-13.

[11] Nosrati A, Zandi Y, Shariati M, Khademi K, Aliabad M, Marto A, Khorami M. “Portland cement structure and its major oxides and fineness.” Smart Struct Syst 22.2 (2018): 425-432. https://doi.org/10.12989/sss.2018.22.4.425

[12] Nuaklong P, Sata V, Chindaprasirt P. “Influence of recycled aggregate on fly ash geopolymer concrete properties.” J Clean Prod 112 (2016): 2300-2307. https://doi.org/10.1016/j.jclepro.2015.10.099

[13] Singh B, et al. “Geopolymer concrete: A review of some recent developments.” Constr Build Mater 85 (2015): 78-90. https://doi.org/10.1016/j.conbuildmat.2015.03.036

[14] Zhuang XY, et al. “Fly ash-based geopolymer: clean production, properties and applications.” J Clean Prod 125 (2016): 253-267. https://doi.org/10.1016/j.jclepro.2016.03.073

[15] Ryu GS, et al. “The mechanical properties of fly ash-based geopolymer concrete with alkaline activators.” Constr Build Mater 47 (2013): 409-418. https://doi.org/10.1016/j.conbuildmat.2013.05.069

[16] Mehdipour S, et al. “Mechanical properties, durability and environmental evaluation of rubberized concrete incorporating steel fiber and metakaolin at elevated temperatures.” J Clean Prod 254 (2020): 120126. https://doi.org/10.1016/j.jclepro.2020.120126

[17] Neupane K, Chalmers D, Kidd P. “High-Strength Geopolymer Concrete- Properties, Advantages and Challenges.” Adv Mater 7.2 (2018): 15-25. https://doi.org/10.11648/j.am.20180702.11

[18] Siddique R, Kaur D. “Properties of concrete containing ground granulated blast furnace slag (GGBFS) at elevated temperatures.” J Adv Res 3.1 (2012): 45-51. https://doi.org/10.1016/j.jare.2011.06.001

[19] Yüksel İ, Siddique R, Özkan Ö. “Influence of high temperature on the properties of concretes made with industrial by-products as fine aggregate replacement.” Constr Build Mater 25.2 (2011): 967-972. https://doi.org/10.1016/j.conbuildmat.2010.06.083

[20] Allahverdi A, Kani EN, Yazdanipour M. “Effects of blast-furnace slag on natural pozzolan-based geopolymer cement.” Ceramics-Silikáty 55.1 (2011): 68-78.

[21] Duan P, Shui Z, Chen W, Shen C. “Enhancing microstructure and durability of concrete from ground granulated blast furnace slag and metakaolin as cement replacement materials.” J Mater Res Technol 2.1 (2013): 52-59. https://doi.org/10.1016/S2238-7854(13)00008-5

[22] Pilehvar S, et al. “Physical and mechanical properties of fly ash and slag geopolymer concrete containing different types of micro-encapsulated phase change materials.” Constr Build Mater 173 (2018): 28-39. https://doi.org/10.1016/j.conbuildmat.2018.03.219

[23] Deb P, Nath P, Sarker P. "Drying shrinkage of slag blended fly ash geopolymer concrete cured at room temperature." Procedia Eng 125 (2015): 594-600. https://doi.org/10.1016/j.proeng.2015.11.066

[24] Mehta PK, Monteiro PJ. "Concrete: microstructure, properties, and materials." McGraw-Hill Education (2014).

[25] Mousavinejad SHG, Rudy B. "Study of Ultrasonic Pulse Wave Velocity in Plain Concrete Using Different Water to Cement Ratio at Different Stress Level." J Civ Environ Eng 50.3 (2020): 37-43. https://doi.org/10.22034/jcee.2020.16382.1404

[26] Ren W, Xu J, Bai E. "Strength and ultrasonic characteristics of alkali-activated fly ash-slag geopolymer concrete after exposure to elevated temperatures." J Mater Civ Eng 28.2 (2016): 04015124. https://doi.org/10.1061/(ASCE)MT.1943-5533.0001395

[27] Hongjian D, Suhuan D, Liu X. "Durability performances of concrete with nano-silica." Constr Build Mater 73 (2014): 705-712. https://doi.org/10.1016/j.conbuildmat.2014.09.042

[28] "IS 13311-1): Method of Non-destructive testing ofconcret, Part 1: Ultrasonic pulse velocity [CED 2: Cement and Concrete]." (1992).

[29] Whitehurst EA. "Soniscope tests concrete structures." J Proc 47.2 (1951).

[30] Kwan WH, Ramli M, Kam KJ, Sulieman MZ. "Influence of the amount of recycled coarse aggregate in concrete design and durability properties." Constr Build Mater 26.1 (2012): 565-573. https://doi.org/10.1016/j.conbuildmat.2011.06.059